OPEN BIOLOGY

royalsocietypublishing.org/journal/rsob

Research

Cite this article: Rack JGM *et al*. 2026 Histidine and tyrosine residues are targets for SIRT6 ADP-ribosylation activity. *Open Biol.* **16**: 250181.
https://doi.org/10.1098/rsob.250181

Received: 29 May 2025
Accepted: 21 January 2026

Subject Areas:
biochemistry

Keywords:
sirtuin, ADP-ribosylation, SIRT6, ADP-ribosyl hydrolases, ARH3, biochemistry, mass spectrometry, nicotinamide adenine dinucleotide (NAD^+), enzyme purification

Authors for correspondence:
Ivan Ahel
e-mail: ivan.ahel@path.ox.ac.uk
Luca Palazzo
e-mail: luca.palazzo@unina.it

†These authors contributed equally to the study.

Electronic supplementary material is available online at https://doi.org/10.6084/m9.figshare.c.8310073.

THE ROYAL SOCIETY PUBLISHING

Histidine and tyrosine residues are targets for SIRT6 ADP-ribosylation activity

Johannes Gregor Matthias Rack[1,†], Evgeniia Prokhorova[2,†], Raffaella Lauro[2,3,†], Anna Georgina Kopasz[2,4,5], Domagoj Baretić[2], Roberto Raggiaschi[2], Jovana Mutabdzija[6], Dmitri V. Filippov[7], Gyula Timinszky[4], Orsolya Leidecker[6,8], Ivan Ahel[2] and Luca Palazzo[9]

[1]Medical Research Council Centre for Medical Mycology at the University of Exeter, Department of Biosciences, Faculty of Health and Life Sciences, Exeter, Devon, EX4 4QD, UK
[2]Sir William Dunn School of Pathology, University of Oxford, Oxford, UK
[3]Department of Translational Medical Sciences, University of Naples Federico II, Naples, Campania, Italy
[4]Institute of Genetics, HUN-REN Biological Research Centre Szeged, Szeged, Csongrád, Hungary
[5]Doctoral School of Multidisciplinary Medical Sciences, University of Szeged, Szeged, Csongrád, Hungary
[6]Institute for Genetics, University of Cologne, Cologne, North Rhine-Westphalia, Germany
[7]Leiden University Institute of Chemistry, Leiden, South Holland, The Netherlands
[8]Max Planck Institute for Biology of Ageing, Cologne, North Rhine-Westphalia, Germany
[9]Molecular Medicine and Medical Biotechnology, University of Naples Federico II School of Medicine and Surgery, Naples, Campania, Italy

IA, 0000-0002-9446-3756; LP, 0000-0002-5556-5549

SIRT6, a highly conserved member of the sirtuin family, plays a critical role in diverse cellular processes, including gene regulation, DNA damage response and maintaining nuclear lamina integrity. These functions are essential in contexts such as differentiation, metabolic regulation, cancer development and ageing. Given the multifaceted influence of SIRT6 on cellular activities, there is an increasing interest in elucidating the regulatory mechanisms governing its enzymatic functions. SIRT6 exhibits two NAD^+-dependent activities: deacetylation and ADP-ribosylation, with current research predominantly focusing on the former. However, the latter—its (ADP-ribosyl)transferase activity—remains underexplored, particularly concerning the specific amino acid targets it modifies and the (ADP-ribosyl)hydrolases that can reverse these modifications. In this study, we have utilized biochemical assays and proteomic techniques to investigate these aspects, revealing that SIRT6 transfers ADP-ribosyl moieties onto histidine and tyrosine residues. In addition, we reveal that the (ADP-ribosyl)hydrolase ARH3 has significant activity in erasing SIRT6-derived ADP-ribosylation in cells.

1. Introduction

ADP-ribosylation is a reversible post-translational modification (PTM) involving the transfer of ADP-ribosyl moieties from NAD^+ to a range of cellular targets, including proteins, nucleic acids and small molecules [1–5]. This modification is predominantly mediated by (ADP-ribosyl)transferases (ARTs), which have diversified into two main superfamilies: the diphtheria toxin-like (ADP-ribosyl)transferases (ARTDs), which include PARPs, the best-studied group of ARTs and the cholera toxin-like (ADP-ribosyl)transferases (ARTCs) [6,7]. While different ARTD members can modify protein substrates on diverse amino acids, such as aspartic/glutamic acids, serine, tyrosine and cysteine, and sometimes nucleic acids [8–12], ARTCs are primarily known to modify protein substrates on arginine residues as well as guanosine bases in nucleic acids [13,14].

Protein ADP-ribosylation facilitates a variety of cellular and physiological processes in vertebrates, including DNA repair, transcription, protein translation, immunity, metabolism and behaviour [2,3,15,16].

As is the case with most protein modifications, protein ADP-ribosylation can be reversed by specific hydrolases, which are categorized into three evolutionarily unrelated families: (ADP-ribosyl)hydrolases (ARHs), macrodomain-containing enzymes (such as MacroD1, MacroD2, TARG1 and PARG) and NADARs ('*NAD*- and *A*DP-*r*ibose'-associated enzymes) that can recognize and hydrolyse different ADP-ribosyl linkages [17,18].

Reversible ADP-ribosylation usually relies on very specific and tightly regulated mechanisms. For example, ADP-ribosylation usually targets specific serine residues in proteins relevant for genome stability during the DNA damage response. This form of ADP-ribosylation is synthesized by the DNA damage-inducible PARPs, PARP1 and PARP2, in complex with their co-regulator HPF1, and the cooperation of ARH3 and PARG reverses the signal [19–24].

In addition to the ART superfamily, other evolutionarily unrelated protein domains can sometimes perform protein ADP-ribosylation. Among these are sirtuins, enzymes primarily known for their NAD^+-dependent deacylase activity [25–30]. They have a conserved catalytic core of approximately 250 amino acids comprising two domains: a Rossmann fold, a mononucleotide binding domain found in many enzymes that bind $NAD(P)^+$/NAD(P)H [31] and a small zinc-binding domain [28,32–35]. The active site is located in a hydrophobic cleft between these two domains, which varies in size and composition between family members, and it facilitates the transfer of an acyl moiety from an acyl-modified substrate onto NAD^+-derived ADP-ribose (ADPr), thereby generating the deacylated substrate, nicotinamide and 2″-*O*-acyl-ADPr, which can be further metabolized to ADP-ribose [27,36–38].

The most compelling example of sirtuins acting as ARTs is the lipoylation-dependent sirtuins (SirTMs) found in pathogenic microorganisms, such as *Staphylococcus aureus* and *Streptococcus pyogenes* [39]. Unlike other classes of sirtuins, SirTMs do not have deacetylase activity. Instead, they mono(ADP-ribosyl)ate aspartic acid residues in their protein target, GcvH-L, to modulate microbial virulence by controlling the response to host-derived reactive oxygen species. A macrodomain-containing protein co-expressed with SirTM from the same operon can efficiently reverse this modification [39,40]. Another example of a sirtuin acting as an ART is represented by *Trypanosoma brucei* Sir2, playing a role in DNA repair and survival [41,42], supporting the hypothesis that there are canonical sirtuins that may possess both deacetylase and ART activities. There have been suggestions in the literature that some sirtuin family members in humans, namely SIRT2, SIRT4, SIRT6 and SIRT7, may also have the ability to ADP-ribosylate proteins in addition to their canonical activities [43–46]. Notably, most research on understanding the protein ADP-ribosylation activity of sirtuins has focused on SIRT6.

SIRT6 is a nuclear sirtuin that regulates cellular processes such as genome stability and energy metabolism [44,47–51]. The enzyme has been suggested to ADP-ribosylate various amino acids, specifically lysine, aspartic acid and arginine residues on several protein substrates. These substrates include PARP1 for the regulation of the DNA damage response [44], the histone demethylase KDM2A [52], the chromatin remodelling protein SMARCA2 [53], the nuclear corepressor protein KAP1 [54], Lamin A/C [55] and the dystrophin repressor Yin Yang 1 (YY1) [56], supporting the role of SIRT6 as a regulator in maintaining genome stability, gene expression and nuclear structure. Despite these findings, the biochemistry, specificity and regulation of SIRT6 ADP-ribosylation remain poorly understood, primarily because direct mass spectrometry (MS)-based evidence for these modifications has been lacking.

Given that MS methods to detect ADP-ribosylation sites in proteins have not been well established until recently, and both lysine and arginine amino acids are prone to non-enzymatic modification [57–59], we performed a more detailed characterization of SIRT6-dependent ADP-ribosylation activity and specificity. We discovered that SIRT6, when recombinantly produced in bacteria or overexpressed in human cells, can efficiently auto-modify tyrosine and histidine residues under certain conditions. We also show that the ARH3 hydrolase can significantly reverse SIRT6-dependent ADP-ribosylation. The findings and tools we developed through this work could pave the way to understanding the mechanism, function and regulation of SIRT6 in the future.

2. Material and methods

2.1. Cell culture

HEK293T (ATCC CRL-3216) cells were acquired from ATCC and grown in DMEM (Sigma) supplemented with 10% FBS (GIBCO) and penicillin-streptomycin (100 U ml^{-1}, GIBCO). HEK293T *HPF1* KO, *ARH3* KO and *PARP1* KO were generated previously and grown as the parental cells [20,21,60]. To induce DNA damage, cells were incubated with 2 mM H_2O_2 (Sigma) in DPBS with calcium and magnesium (GIBCO) for 10 min. For PARP inhibition, cells were pretreated with 1 µM Olaparib (Cayman Chemical) for 1 h, and Olaparib was added to the DPBS solution in the case of subsequent DNA damage induction.

2.2. Immunoblotting

Cells were lysed with ice-cold Triton X-100 lysis buffer (50 mM TrisHCl [pH 8.0], 100 mM NaCl, 1% (v/v) Triton X-100) supplemented with 5 mM $MgCl_2$, protease and phosphatase inhibitors (Roche), 2 µM Olaparib (Cayman Chemical), 2 µM PARGi PDD00017273 (Sigma) and 2 µM Trichostatin A (Sigma). Lysates were incubated with 0.1% Benzonase (Sigma) for 30 min at 4°C, centrifuged at 14 000 r.p.m. for 15 min, and supernatants were collected for analysis. Protein concentrations were determined using Bradford Protein Assay (Bio-Rad). Normalized samples were boiled in 1 x NuPAGE LDS sample buffer (Invitrogen) with 10 mM TCEP (Sigma), resolved on NuPAGE Novex 4–12% Bis-Tris gels (Invitrogen) and transferred onto

nitrocellulose membranes (Bio-Rad) using Trans-Blot Turbo Transfer System (Bio-Rad). The membranes were blocked in PBS buffer with 0.1% (v/v) Tween 20 and 5% (w/v) skimmed dried milk (Premier Foods plc, UK) for 1 h at room temperature and incubated overnight with primary antibodies (1 : 1000, unless stated otherwise) at 4°C, followed by 1 h incubation with peroxidase-conjugated secondary anti-mouse (Agilent, P0447, 1 : 3000) or anti-rabbit (Agilent, P0399, 1 : 3000) antibody at room temperature. Rabbit anti-pan-ADPr (MABE1016; 1 : 1500), mono-ADPr (MABE1076, 1 : 1000), anti-histone H3 (07–690, 1 : 5000) and mouse anti-PARP2 (MABE18, 1 : 500) antibodies were from Millipore, rabbit anti-ARH3/ADPRHL2 (HPA027104; 1 : 2000) from Atlas Antibodies, and rabbit anti-PARP1 (ab32138; 1 : 2000) and anti-GFP (ab290, 1 : 3000) from Abcam.

2.3. Construction of plasmids and site-directed mutagenesis

The expression vector for PARP14 WWE-ART was described previously [61]. The coding sequence of human SIRT6 was obtained in pDONR221 from DNASU plasmid repository (HsCD00042070), and a 'TAG' stop codon was inserted via PCR-based site-directed mutagenesis using the QuickChange Lightning kit (Agilent). For His-affinity purification, the coding sequence was transferred into pDEST17, and for expression of YFP-tagged SIRT6 in HEK293T cells, into pDEST-YFP via gateway cloning (Life Technologies). All indicated mutations were introduced via PCR-based site-directed mutagenesis using the QuickChange Lightning kit (Agilent).

2.4. Protein expression and purification

Recombinant 6xHis-SIRT6 was expressed in Rosetta (DE3) cells grown in LB medium supplemented with 1% (w/v) D-glucose, ampicillin (100 µg ml^{-1}) and chloramphenicol (34 µg ml^{-1}). Expression cultures were inoculated 1 : 100 with overnight cultures and grown at 37°C to OD_{600} 0.6. Cultures were cooled on ice to approximately 20°C and expression was induced by the addition of 0.4 mM ITPG and 5 µM zinc acetate. Cells were grown at 18°C overnight and harvested by centrifugation. Pellets were resuspended in lysis buffer (50 mM TrisHCl [pH 7.5], 500 mM NaCl, 20 mM imidazole) and stored at −20°C until purification.

For purification, thawed pellets were incubated with benzonase and lysozyme for 1 h on a rotating wheel at 4 °C and subsequently lysed by incubation with 1× BugBuster (Millipore) for 30 min and a rotating wheel at 4°C. Insoluble material was removed by centrifugation and supernatant incubated with Ni^{2+}-NTA agarose (SERVA Electrophoresis GmbH) for 1 h on a rotating wheel at 4°C. The reaction was applied to a gravity column, and the resin was washed with lysis buffer, followed by wash buffers A and B (lysis buffer containing 50 mM [A] and 80 mM [B] imidazole, respectively). Remaining proteins were eluted using elution buffer (50 mM Tris-HCl [pH 7.5], 300 mM NaCl, 250 mM imidazole) and dialysed overnight against storage buffer (50 mM Tris-HCl [pH 7.5], 200 mM NaCl, 1 mM DTT, 5% (v/v) glycerol).

PARP14 WWE-ART was expressed and purified as described previously [61].

2.5. Enzymatic assays

Auto-MARylation of SIRT6 and of the PARP14 fragment containing WWE and ART domain (WWE-ART) was carried out for 1 h at 37 °C in MARylation buffer (50 mM TrisHCl [pH 8], 200 mM NaCl, 10 mM $MgCl_2$, 1 mM DTT) using 5 µM (ADP-ribosyl)transferase and supplemented with 200 µM NAD^+ as indicated [62]. Reactions were halted by adding LDS sample buffer (Invitrogen), or they were further incubated with ADP-ribosyl hydrolases. De-modification assays were performed using each hydrolase at a final concentration of 1 µM. The reactions were allowed to proceed for 1 h before being stopped with the LDS sample buffer. All reactions were analysed by immunoblotting using rabbit anti-pan-ADPr (MABE1016; dilution 1 : 5000).

2.6. Transfection and immunoprecipitation

HEK293T cells were plated in 100 mm tissue culture dishes and transfected with YFP-SIRT6 or YFP (empty vector control) expression vectors for 24 h using Polyfect (QIAGEN) following the manufacturer's instructions. The cells were washed with PBS and lysed as described above. Normalized cell lysates were incubated with GFP-Trap MA magnetic agarose beads (ChromoTek) for 2 h while rotating at 4°C. The beads were washed with Triton X-100 lysis buffer five times and eluted with 2 × NuPAGE LDS sample buffer (Invitrogen) with TCEP (Sigma). The samples were then analysed using western blotting. For MS analysis, YFP-SIRT6 was immunopurified using GFP-trap nanobodies, followed by SDS-PAGE separation and staining with Sypro Ruby (Life Technology). The relevant protein band was excised and subsequently processed for analysis via MS.

2.7. In gel digestion

Cellular SIRT6 digestion was performed using in-gel tryptic digestion. Gel slices were washed with 200 µl H_2O at 26°C for 5 min, then centrifuged to remove excess liquid. The gel pieces were destained with acetonitrile (ACN), then dried in a vacuum centrifuge for 10 min. Rehydration involved adding 5 µl of Buffer 1 (50 mM ammonium bicarbonate (ABC) + trypsin), incubated at 4°C for 10 min, followed by 50 µl of Buffer 1, incubated on ice for 20 min. The solution was removed carefully, and 50 µl of Buffer 2 (50 mM ABC) was added. The samples were then incubated overnight at 37°C. Peptides were extracted by centrifugation, followed by three extraction steps: adding 150 µl of extraction solution (47.5% (v/v) ACN, 47.5% (v/v) water,

5% (v/v) formic acid (FA)), sonication for 15 min, then collecting the solution; adding 100 µl of ACN, sonication and collection. Pooled extracts were dried via SpeedVac vacuum concentrator overnight. Dried peptides were resuspended in 30 µl of 0.1% (v/v) FA and purified using an in-house fabricated C18 reverse-phase tip, eluted with two rounds of 30 µl of 60% (v/v) ACN for MS analysis.

2.8. *In vitro* ADP-ribosylation assay with recombinant SIRT6 and protein digestion

Recombinant 6× His-SIRT6 (10 µg) was incubated in 50 mM TrisHCl (pH 8.0) and 150 mM NaCl with or without 200 µM NAD^+ for 1 h at 37°C. Reactions were stopped with the addition of 8 M urea and processed using a FASP (filter-aided sample preparation) protocol: samples were loaded onto Vivacon 30 kDa ultrafiltration units, alkylated and buffer was exchanged to ABC. Trypsin in ABC (enzyme : protein, 1 : 100) was added, mixed and incubated overnight at 37°C. Peptides were recovered by centrifugation, acidified and then desalted using an in-house fabricated C18 reverse-phase tip. After binding, the samples were eluted with 60% (v/v) ACN/0.1% (v/v) FA and dried in a SpeedVac vacuum concentrator.

2.9. Mass spectrometry analysis

All samples were analysed on an Orbitrap Fusion instrument (Thermo), coupled to an EASY-nLC. Peptides were resolved in a 120 min gradient (flow 200 nl min^{-1}) on a Picofrit C18 column from New Objective (75 µm inner diameter × 25 cm, 1.9 µm particle size, 120 Å pore size). The Orbitrap Fusion was operated in a Data Dependent Acquisition mode using ETD fragmentation. MS resolution was set to 120K with a scan range 300–1500 *m/z*, and the AGC (automatic gain control) target value was 1 000 000 ions with dynamic exclusion of 15 s. The top 10 most intense ions were fragmented using ETD with a maximum injection time of 500 ms, a target value of 500 000 and a resolution of 30K. Raw files were analysed with MaxQuant (v. 2.4.12.0) with enzyme specificity set to trypsin, allowing for up to four missed cleavages. Cysteine carbamidomethylation was set as a fixed modification, and methionine oxidation; protein *N*-acetylation; ADP-ribosylation (mass shift of 541.0611; composition $C_{15}H_{21}N_5O_{13}P_2$) on all residues were used as variable modifications.

3. Results

3.1. Recombinant SIRT6 auto-ADP-ribosylates on histidine *in vitro*

A previous study explored the (ADP-ribosyl)transferase activity of SIRT6 [63], but the amino acid specificity of this reaction remains elusive to date. To gain insights, we purified full-length human SIRT6, alongside two previously established catalytic mutants, N114A and H133Y [63–66], from *Escherichia coli* and analysed the ADP-ribosylation status of these proteins. Notably, immunoblot analysis using an anti-pan-ADP-ribose binding reagent showed that wild-type SIRT6, but not the catalytic mutants, is substantially ADP-ribosylated even in the absence of exogenous NAD^+ (figure 1A). This suggests an intrinsic catalytic activity of SIRT6 within the bacterial cytoplasm. In contrast, the purified catalytic domain of PARP14 [62], produced in *E. coli* under conditions similar to those of SIRT6, exhibited no detectable modification. However, the robust enzymatic auto-modification of PARP14 can be readily achieved *in vitro* by adding exogenous NAD^+ to the protein preparation (figure 1A). In contrast, the auto-modification of SIRT6 showed only a modest increase upon addition of NAD^+ (figure 1B). This suggests either that SIRT6 achieves a near-complete auto-modification in the bacterial cytoplasm or that SIRT6 ADP-ribosylation requires very specific reaction conditions that are not simulated by our reaction buffer.

To assess the type of ADP-ribosyl linkage catalysed by SIRT6, we performed MS analysis of recombinant wild-type SIRT6 with or without additional NAD^+ treatment. To accurately identify the modified residues, we employed ETD fragmentation, which is optimal for preserving labile PTMs like ADP-ribose on amino acids, thereby enabling more precise and confident localization of the modification sites [67]. MS analysis of SIRT6 in the absence of NAD^+ revealed no ADP-ribosylated residues within the SIRT6 protein sequence, but significant modification of histidine residues within the 6×His-tag used to purify the recombinant protein (figure 1C; electronic supplementary material, figure S1A–C). Treatment with NAD^+ prior to MS analysis led to the detection of SIRT6 residues His68 and His342 as ADP-ribosylated (figure 1D,E; electronic supplementary material, figure S2A). His342 is located in the *C*-terminal domain and was previously identified in a large-scale human ADP-ribosylome analysis [68]. His68 is located in the Rossmann Fold domain of SIRT6 (figure 1F), and its ADP-ribosylation has never been detected before. His68 is surface-accessible (figure 1G), while His342 is located within an unstructured part of the protein. Hence, both residues are accessible for enzymatic modification. Interestingly, both residues also share similar amino acids preceding the modified sites, glycine and proline for His68 (GPH) and alanine and proline for His342 (APH), respectively, suggesting a potential sequence motif for modification.

To further confirm that His is the primary target for SIRT6 ADP-ribosylation activity and further address the biochemistry of this modification, we treated auto-modified SIRT6 with a panel of different (ADP-ribosyl)hydrolases, namely, the serine- and tyrosine-(ADP-ribosyl)hydrolase ARH3 [11,20], aspartate-/glutamate-(ADP-ribosyl)hydrolases MacroD1 [37,69–71], MacroD2 [69,70], TARG1 [72] and PARP9 macrodomain 1 [73]. In addition, we assessed the human poly(ADP-ribose) glycohydrolase (hPARG), which cleaves ADP-ribose polymers [24,74], *Drosophila melanogaster* PARG (dmPARG) that is capable of cleaving serine-mono(ADP-ribosylation) [75], and phosphodiesterase NUDT16, a pyrophosphohydrolase capable of cleaving the phosphodiester bond between the ribose-5′-phosphate and AMP moieties both in ADP-ribosyl polymers as well as in

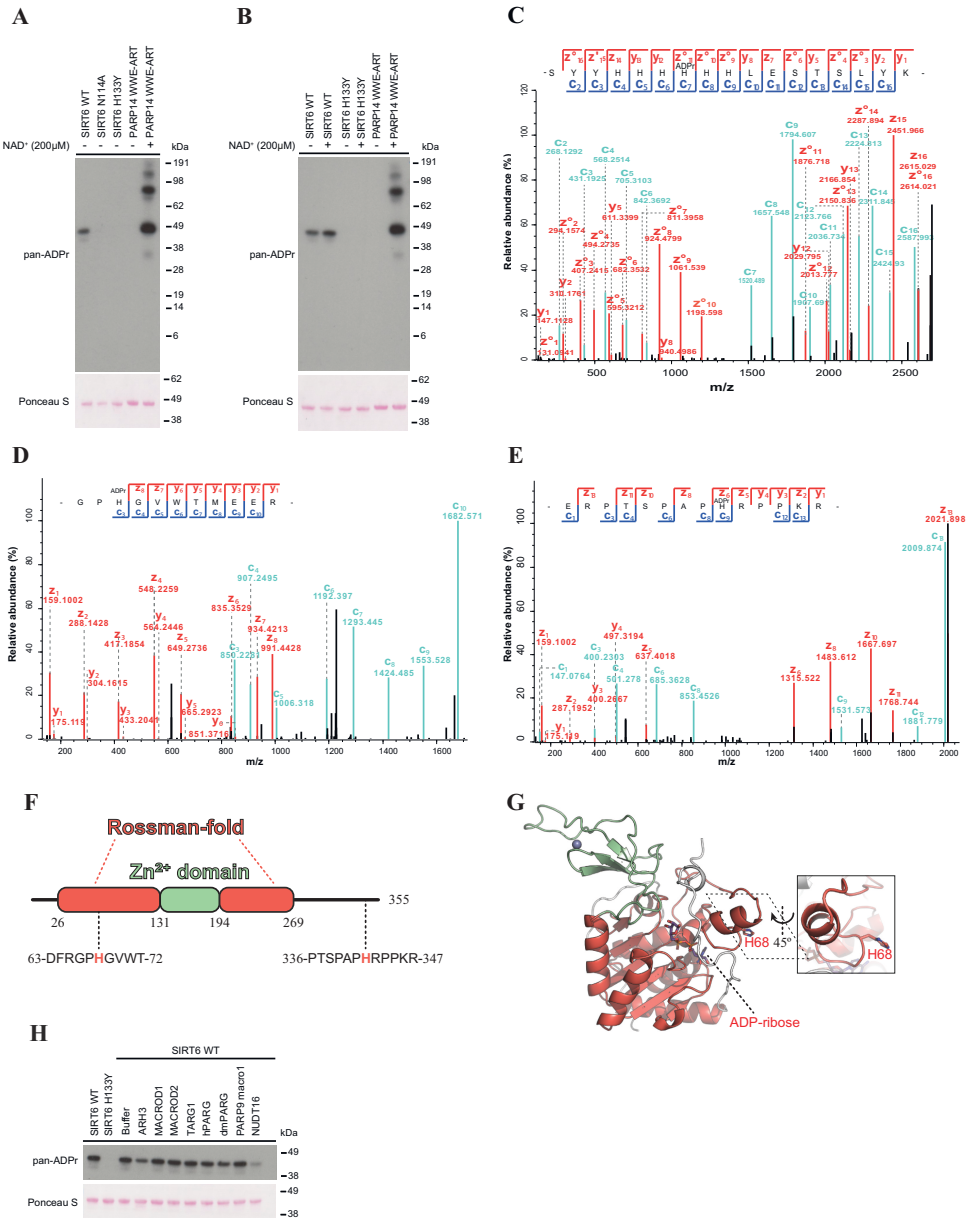

Figure 1. Auto-ADP-ribosylation of SIRT6 occurs on histidine residues *in vitro*. (A,B) Immunoblot analysis of recombinant 6xHis-SIRT6 WT, N114A and H133Y mutant. ADP-ribosylation levels were assessed using the pan-ADP-ribosylation (pan-ADPr, MABE1016) antibody. Samples were pre-incubated in the presence or absence of NAD^+ as indicated. PARP14 catalytic fragment (WWE-ART domains) served as a positive control, and Ponceau S staining was used as a loading control. (C) MS/MS ETD spectrum of recombinant SIRT6 without additional NAD^+ treatment shows ADP-ribosylation on the fourth histidine residue within the hexahistidine-tag. (D,E) MS/MS ETD spectra of recombinant SIRT6 after NAD^+ treatment show ADP-ribosylation of His68 (D) and His342 (E). (F) Schematic representation of the SIRT6 domain architecture with identified ADP-ribosylation sites depicted below the scheme. Domain boundaries were inferred from structural information. (G) AlphaFold 3 model of SIRT6 in complex with ADP-ribose (from PDB 3K35). The model closely resembles the earlier solved SIRT6:ADP-ribose structure (PDB 3K35; r.m.s.d. of 0.183 Å for 237 C^α atoms) and fills gaps in the experimental electron density. The positioning of His68 is highlighted in the close-up, and the structure is coloured as shown in the scheme in (G). For clarity, the unstructured C-terminal region was omitted. (H) Demodification of auto-ADP-ribosylated SIRT6 by known human hydrolases was assessed by immunoblotting using a pan-ADP-ribosylation antibody (pan-ADPr; MABE1016). The catalytically inactive SIRT6 H133Y mutant served as a negative control, and Ponceau S staining was used as a loading control.

monomers, independent of the substrate-attachment linkage [76]. As illustrated in figure 1H most of the (ADP-ribosyl)hydrolases did not show hydrolytic activity against SIRT6 auto-modification, with the exceptions of NUDT16 and ARH3. The activity of NUDT16 is expected, as it can hydrolyse the phosphodiester bond within the ADP-ribose linked to proteins, regardless of the type of ADP-ribosyl linkage [76]. On the other hand, ARH3 displays minor but notable activity in this context, consistent with previous findings that highlight its modest activity against ADP-ribosylated histidine residues [77,78].

3.2. SIRT6 auto-ADP-ribosylates in cells

To evaluate SIRT6 auto-modification activity in human cells in the context of DNA damage, we overexpressed YFP-tagged SIRT6 in HEK293T cells, exposed or not to hydrogen peroxide (H_2O_2) as a source of DNA damage. We then visualized ADP-ribosylated proteins in both total extracts and via YFP immunoprecipitation (figure 2A). Notably, a strong ADP-ribosylation signal was observed at approximately 62 kDa, corresponding to YFP-tagged SIRT6, in both input and immunoprecipitated

samples (indicated by an arrow infigure 2A, left panel). This signal was absent in cells transfected with the YFP empty vector and was independent of DNA damage. In contrast, a 98 kDa band detected in the anti-pan-ADP-ribosylation immunoblot corresponds to PARP1 and was observed only in DNA-damaged cells. Additionally, the signal for this ADP-ribosylated protein was lost entirely in cells transfected with YFP-tagged catalytic mutants of SIRT6, suggesting that the ADP-ribosylation detected corresponded to auto-modified SIRT6. To further confirm this, we replicated these experiments in *HPF1* knock-out (KO) HEK293T (figure 2B). HPF1 is an accessory factor for PARP1 and PARP2, essential for catalysing the ADP-ribosylation of serine residues (Ser-ADPr) in target proteins [19–21,60,79,80]. This type of ADP-ribosylation is one of the most abundant chemical modifications catalysed by PARP1 and PARP2 in response to DNA damage [21,81]. YFP-SIRT6 modification was not affected by *HPF1* gene depletion, indicating that it is probably independent of PARP1/2:HPF1 complex activity (figure 2B). The hypothesis that SIRT6 ADP-ribosylation is independent of PARP1/2:HPF1 complex activity during DNA damage is further supported by the persistence of ADP-ribosylation in YFP-SIRT6 (figure 2C) and *C*-terminally GFP-tagged SIRT6 (electronic supplementary material, figure S3A) in *PARP1* KO HEK293T cells, as well as in parental HEK293T cells treated with Olaparib, a PARP1/2 inhibitor. Notably, ADP-ribosylation of YFP-SIRT6, as well as GFP-tagged SIRT6, appeared to be influenced by *ARH3* KO [11,17,20,23,80], whose depletion increased SIRT6 ADP-ribosylation (figure 2C; electronic supplementary material, figure S3A), thus providing further support for the role of ARH3 in reversing SIRT6-mediated ADP-ribosylation.

3.3. SIRT6 is auto-ADP-ribosylated at histidine and tyrosine sites in cells

To identify the amino acid linkage associated with SIRT6 auto-modification in HEK293T cells, we performed MS analysis of YFP-tagged SIRT6 immunoprecipitated from *ARH3* KO cells to enrich for the ADP-ribosylation sites.

This identified two significant ADP-ribosylation sites in YFP-SIRT6: Tyr245, part of the linker between the YFP-tag and the SIRT6 opening reading frame (figure 3A; electronic supplementary material, figure S2A), and His68 in the SIRT6 sequence (figure 3B, C), which we previously detected in recombinant auto-modified SIRT6 (figure 1E). This indicates that SIRT6 His68 is probably a genuine auto-modification site. In contrast, we could not detect SIRT6 His342 ADP-ribosylation, which was observed *in vitro* (figure 1F).

To explore the mechanisms of ADP-ribosylation in SIRT6, we conducted immunoprecipitation assays on control YFP protein, wild-type YFP-SIRT6 and point mutants of the previously identified ADP-ribosylation sites (tag(Y245A)-SIRT6(wild type), tag(wild type)-SIRT6(H68A) and tag(wild type)-SIRT6(H342A) (figure 3D). Notably, analysis with a pan-ADP-ribosylation antibody indicated that the tag(Y245A) mutation abolished SIRT6 auto-modification in cells. In contrast, the SIRT6 H68A and H342A mutations did not significantly influence the anti-ADP-ribosylation signal, suggesting relatively low levels of ADP-ribosylation at these sites. Altogether, these results indicate that the tyrosine modification within the YFP tag is the primary SIRT6-dependent ADP-ribosylation site in this system.

4. Discussion

SIRT6 is an NAD^+-dependent enzyme with well-characterized deacylase activity [25–30] that has repeatedly been suggested to moonlight as a mono(ADP-ribosyl)transferase [25,28,35,82]. SIRT6 plays a crucial role in several cellular pathways, such as chromatin condensation and the transcriptional regulation of various gene networks, thus indirectly affecting processes such as glucose metabolism, differentiation, DNA repair, NF-κB signalling, tumorigenesis, early development and ageing [34,83–90]. Although the deacetylase activity of SIRT6 may account for many of its cellular and biological functions, its comparatively poorly studied ART activity may also be important at the organism level. For example, SIRT6 alleles, such as one with the double substitution N308K/A313S, are associated with increased ART activity and weakened deacylase activity. These alleles have been linked to longevity and enhanced DNA repair capabilities *in vitro* [55]. SIRT6 was mainly suggested to ADP-ribosylate protein substrates at lysine residues. For example, mono(ADP-ribosyl)ation of PARP1 at Lys521 by SIRT6 was suggested to contribute to its enzymatic activation in response to oxidative stress [44]. In addition, SIRT6-dependent lysine ADP-ribosylation of BAF170/SMARCA2 was reported to control transcription [53]. However, it has historically been challenging to identify ADP-ribosylation sites reliably: in particular, lysine residues are prone to nonenzymatic modification by free ADP-ribose *in vitro* and *in cellulo* [57–59]. To overcome these challenges, we employed ETD fragmentation in our MS analysis, which has resulted in the superior identification of ADP-ribosylation sites [67]. Utilizing this technique, we observed modifications of the hexahistidine tag and His68 in recombinant SIRT6, as well as Tyr245 at the end of the YFP tag and His68 of the SIRT6 open reading frame in cellularly expressed SIRT6. We could exclude nonenzymatic modification under expression conditions by introducing a mutation of the ADP-ribosylation site Tyr245 in YFP-SIRT6 (figures 2A and 3D).

Structurally, SIRT6 differs from other sirtuins: it lacks the cofactor binding loop, can bind NAD^+ in the absence of an acyl-substrate and has an elongated acyl binding channel, which also allows accommodation of long-chain acyl moieties such as myristoyl and palmitoyl groups [26,27,30,91]. Furthermore, the *N*-terminus of SIRT6 can fold towards the active site to stabilize the binding of long-chain fatty acid-modified substrates, thereby increasing the efficiency of the de-modification reaction [27]. Therefore, it is feasible that in the absence of a deacylation substrate, the *N*-terminal tags may be positioned near the NAD^+-occupied active site, thus increasing the likelihood of ADP-ribosyl transfer to occur. This would account for the observed modification of the linker region following the YFP tag as well as the hexahistidine tag of recombinant SIRT6 (figures 1C and 3A; electronic supplementary material, figure S1A–C).

It is interesting to note that SIRT6 is not only capable of binding NAD^+ in the absence of a substrate but also increases the rate of spontaneous NAD^+ hydrolysis. This suggests that the glycosidic bond in the SIRT6:NAD^+ complex is weakened, allowing the

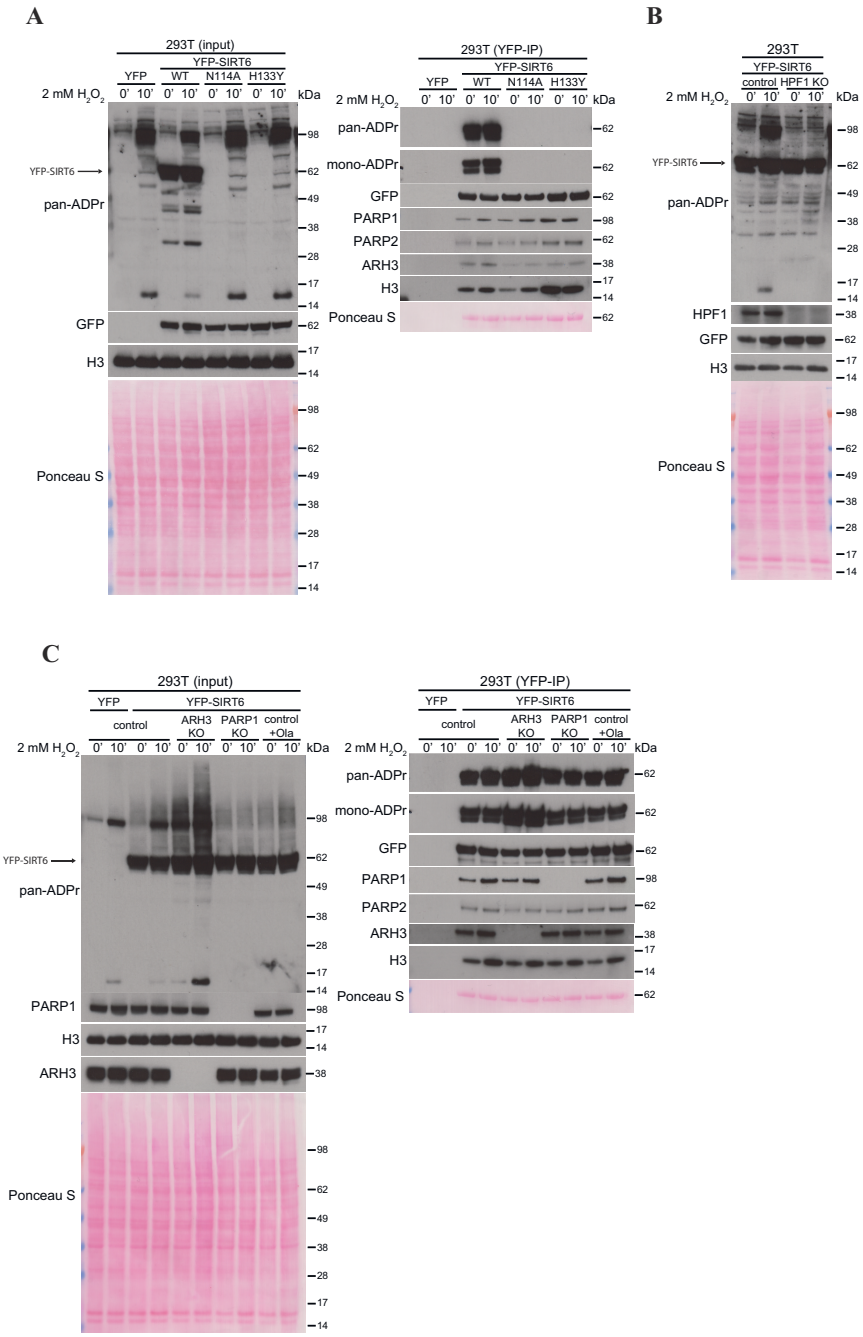

Figure 2. The SIRT6 auto-ADP-ribosylation in cells is affected by ARH3 knock-out. (A) Immunoblot analysis assessing the ADP-ribosylation of transgenic SIRT6 WT, mutants and YFP control (YFP) expressed in HEK293T cells treated or not (0′) with 2 mM of H_2O_2 for 10 minutes. Ponceau S staining was utilized as a loading control. (B) Immunoblot analysis assessing the impact of HPF1 on transgenic YFP-SIRT6 auto-ADP-ribosylation when expressed in *HPF1* knock-out (KO) or isogenic HEK293T cells. The cells were treated or not (0′) with 2 mM H_2O_2 for 10 min. Ponceau S staining was used as a loading control. (C) Immunoblot analysis assessing the impact of ARH3 and PARP1 on transgenic YFP-SIRT6 auto-ADP-ribosylation expressed in *ARH3* KO, *PARP1* KO or isogenic HEK293T control cells treated or not with 1 µM Olaparib (Ola). Cells were treated or not (0′) with 2 mM of H_2O_2 for 10 min. Ponceau S staining and histone H3 detection were used as loading controls.

formation of a reactive intermediate, such as an oxocarbenium ion. In the absence of an ADPr acceptor, this intermediate would revert unproductively to NAD^+ but may persist long enough to react with a suitable acceptor. This notion is further supported by a deposited structure of a SIRT6:ADP-ribose:nicotinamide complex, which shows movement of the distal ribose towards the substrate binding site (ribose C1″–nicotinamide N1 distance 7.9 Å), indicating (i) flexibility of the ADP-ribose after glycosidic bond cleavage and (ii) positioning of the ribose α-face towards the substrate, consistent with the expected reaction geometry.

Together, these observations support the idea that glycosidic bond cleavage can occur spontaneously and that the resulting intermediate is suitably positioned to react with an acceptor residue within the active site. The tyrosine modification site identified in the flexible tag region of the ectopically expressed SIRT6 in cells is not a natural site but is nonetheless strongly modified, suggesting that robust *trans*-ADP-ribosylation of endogenous proteins may occur under certain cellular conditions. Under physiological conditions, the formation of stable or transient protein complexes could further facilitate such reactions by increasing contact times, thereby creating an environment in which SIRT6-mediated ADP-ribosylation can occur more efficiently on the target proteins. Our data reveal only histidine and tyrosine residues as SIRT6 targets, which is in line with a recent study identifying histidine-rich regions as SIRT6 ADP-ribosylation targets [82], albeit without providing proof that

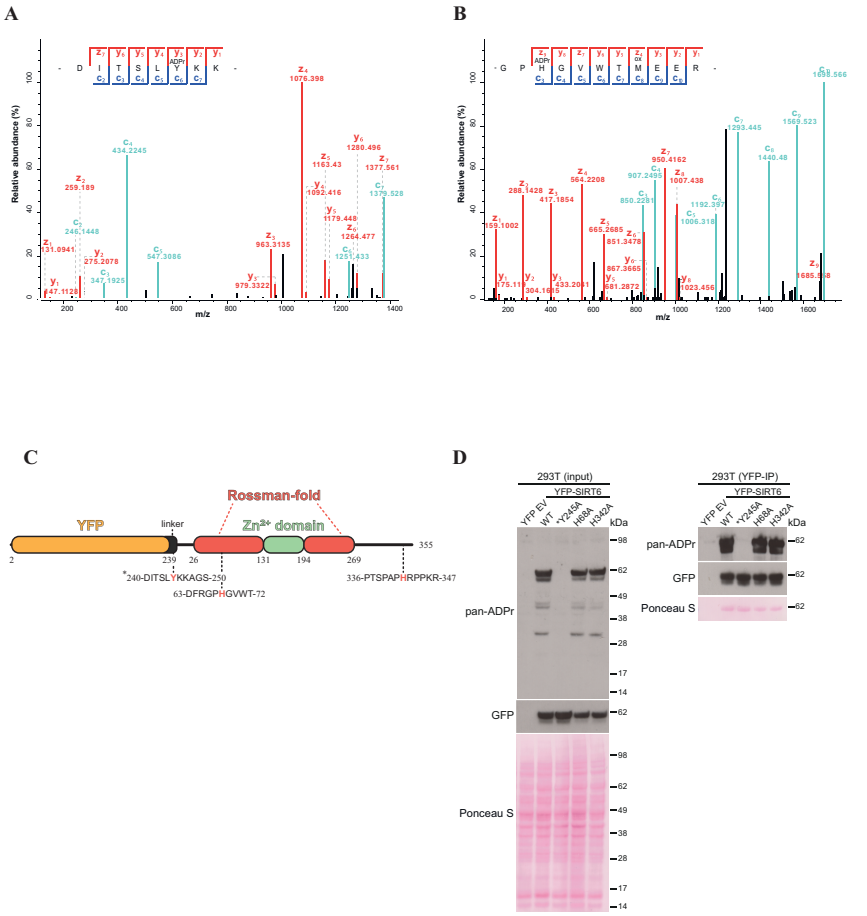

Figure 3. SIRT6 auto-ADP-ribosylates in cells on histidine and tyrosine residues. (A) The MS/MS ETD spectrum of YFP-SIRT6 from ARH3 KO U2OS cells indicates ADP-ribosylation of Tyr245 in the YFP-tag (attB1-derived linker). (B) MS/MS ETD spectrum of YFP-SIRT6 isolated from *ARH3* KO U2OS cells shows ADP-ribosylation of His68 (SIRT6). (C) Schematic representation of the YFP-SIRT6 domain architecture with identified ADP-ribosylation sites depicted below the scheme. Domain boundaries were inferred from structural information. The asterisk denotes the sequence in the YFP linker that undergoes ADP-ribosylation. (D) Immunoblot analysis assessing the impact of ADP-ribosylation site mutation on overall protein ADP-ribosylation when expressed in HEK293T cells. Ponceau S staining served as the loading control. The asterisk indicates that the tyrosine at position 245, which was mutated to alanine (Y245A), is located within the YFP linker and not within the SIRT6 amino acid sequence.

histidine residues are modified. This suggests that the microenvironment of the ADP-ribosyl acceptor site also has an influence on reaction efficiency, e.g. by altering the local pK_a of the acceptor. However, further mechanistic investigations are needed to elucidate the molecular details of the reaction.

Observation of tyrosine and histidine ADP-ribosylation also aligns with previous ADP-ribosylomics studies, which revealed the presence of histidine and tyrosine ADP-ribosylation in cells, but for the most part could not identify the ART(s) responsible for ADP-ribosylation [68,81,92]. The proteins identified as tyrosine or histidine ADP-ribosylated are largely involved in non-DNA damage-related processes, such as transcription, metabolism and cell motility, among others [11,68,81,92–94]. Such an overlap with pathways regulated by SIRT6 suggests that some of these proteins may be substrates of SIRT6. Therefore, future studies will need to elucidate the full extent of SIRT6-mediated ADP-ribosylation, which may reveal important and previously unexplored roles in regulating essential cellular processes. In line with this, our data showed no significant increase in global auto-ADP-ribosylation of SIRT6 following hydrogen peroxide treatment. However, this does not exclude the possibility of regulated modifications occurring in the context of DNA damage at specific residues on SIRT6 itself or on its protein substrates. This may be somewhat analogous to the case of PARP1 and PARP2, where interaction with HPF1 shifts ADP-ribosylation specificity from glutamic and aspartic acids to serine residues in response to DNA damage [22,95].

Beyond the establishment of the modification, the dynamic regulation of cellular processes by PTMs, including ADP-ribosylation, requires these modifications to be reversible. Previous studies on synthetic peptides with modified histidine or histidine mimetics indicated that ARH3 has a modest activity against close isosteres of histidine ADP-ribosylation [78]. In accordance, we observed that ARH3 can, albeit not very efficiently, hydrolyse auto-ADP-ribosylation of hexahistidine-tagged SIRT6. Similarly, in *ARH3* KO cells, we observe an enhancement in SIRT6 ADP-ribosylation levels. This suggests that ARH3 may play a crucial role in the dynamic regulation of SIRT6-derived histidine modifications. Our previous work suggests that both ARH3 and PARG can cleave tyrosine-ADP-ribosylation very efficiently [11]. This makes both enzymes excellent candidates for further investigation of the role of SIRT6 in establishing tyrosine-ADP-ribosylation marks. To this end, our results suggest that our SIRT6 systems (both recombinant and cell culture) are promising tools for investigating which enzymes may hydrolyse histidine- and tyrosine-ADP-ribosylation linkages and gaining insights into the regulation of these modifications. The screen for enzymes involved in reversing His- and Tyr-ADP-ribosylation may benefit from having recombinant substrates

ADP-ribosylated *in vitro* by SIRT6 rather than peptides of chemical synthesis. Furthermore, investigating SIRT6's auto-modification could serve as a novel, straightforward and cost-effective method to evaluate chemical modulators that specifically affect SIRT6's ADP-ribosylation activity. Finally, our work provides the first system with a defined tyrosine-ADP-ribosylated site in cells.

Altogether, this study represents an important step in clarifying SIRT6's ART activity and delivers a novel framework for exploring molecules and enzymes that modulate its activity, using SIRT6 auto-modification as an *in vitro* model.

Ethics. This work did not require ethical approval from a human subject or animal welfare committee.

Data accessibility. Plasmids and cell lines generated/utilized in this study are available to the lead contact upon request. The data supporting this study's findings are included in the article. Nevertheless, upon request, the lead contact can provide any additional information, including MS raw data, required to re-analyse the data reported in this manuscript.

Supplementary material is available online [96].

Declaration of AI use. We have not used AI-assisted technologies to create this article, except for the model of SIRT6 in complex with ADP-ribose (from PDB 3K35), shown in figure 3G, which was generated by AlphaFold 3.

Authors' contributions. J.G.M.R.: conceptualization, data curation, formal analysis, funding acquisition, investigation, supervision, validation, visualization, writing—review and editing; E.P.: data curation, investigation, validation, visualization, writing—review and editing; R.L.: investigation; A.G.K.: data curation, investigation, validation, visualization, writing—review and editing; D.B.: data curation, investigation, validation, visualization, writing—review and editing; R.R.: investigation; J.M.: data curation, visualization; D.V.F.: conceptualization, writing—review and editing; G.T.: conceptualization, supervision, writing—review and editing; O.L.: data curation, investigation, visualization, writing—review and editing; I.A.: conceptualization, funding acquisition, project administration, supervision, writing—original draft, writing—review and editing; L.P.: conceptualization, data curation, formal analysis, funding acquisition, project administration, supervision, writing—original draft, writing—review and editing.

All authors gave final approval for publication and agreed to be held accountable for the work performed therein.

Conflict of interest declaration. We declare we have no competing interests.

Funding. We acknowledge funding from: European Union—Next Generation EU, National Recovery and Resilience Plan (NRRP), Mission 4, Component 1, CUP F53D23003840006. PRIN—Progetti di Ricerca di Interesse Nazionale—Bando 2022—Prot. 2022R85H27 to L.P.; Ovarian Cancer Research Alliance (813369) to LP and IA; Wellcome Trust (210634, 223107, 302632) to I.A.; Cancer Research United Kingdom (C35050/A22284) and Biotechnology and Biological Sciences Research Council (BB/R007195/1 and BB/W016613/1) to I.A. Max Planck Society and the Deutsche Forschungsgemeinschaft (DFG, German Research Foundation) under Germany's Excellence Strategy (CECAD, EXC 2030-390661388) and project number 524909464 to O.L. O.L. further acknowledges funding from the CMMC (CAP 30), the RTG2550 and the FOR5504. We would like to thank Thomas Colby for help with mass spectrometric data analysis. J.G.M.R. acknowledges funding from the MRC Centre for Medical Mycology at the University of Exeter (MR/N006364/2 and MR/V033417/1), the NIHR Exeter Biomedical Research Centre (NIHR203320). Additional work may have been undertaken by the University of Exeter Biological Services Unit. The views expressed are those of the author(s) and not necessarily those of the NIHR or the Department of Health and Social Care. J.G.M.R. laboratory is supported by the Medical Research Council (MR/X007472/1). K.P. is supported by a European Molecular Biology Organization (EMBO) Postdoctoral Fellowship (ALTF 733-2024). A.G.K. was supported by the Eötvös Predoctoral Fellowship provided by the Hungarian government. R.L. is supported by a fellowship funded by the European Union—Next Generation EU, National Recovery and Resilience Plan (NRRP), Mission 4, Component 2, Investment 1.1, CUP E53D23009840006, PRIN—Progetti di Ricerca di Interesse Nazionale—Bando 2022—Prot. 2022CSYK9L. The funding bodies had no role in the study's design, data collection, analysis, interpretation or manuscript writing.

Acknowledgements. We thank the MPI AGE Proteomics Core Facility (Cologne, Germany) for providing instrumentation and Thomas Colby for helpful discussions on the data analysis. R.L. and L.P. thank Nella Prevete and Rosa Marina Melillo (University of Naples) for helpful discussions and encouragement.

References

1. Palazzo L, Mikoč A, Ahel I. 2017 ADP-ribosylation: new facets of an ancient modification. *Febs J.* **284**, 2932–2946. (doi:10.1111/febs.14078)
2. Suskiewicz MJ, Prokhorova E, Rack JGM, Ahel I. 2023 ADP-ribosylation from molecular mechanisms to therapeutic implications. *Cell* **186**, 4475–4495. (doi:10.1016/j.cell.2023.08.030)
3. Gupte R, Liu Z, Kraus WL. 2017 PARPs and ADP-ribosylation: recent advances linking molecular functions to biological outcomes. *Genes Dev.* **31**, 101–126. (doi:10.1101/gad.291518.116)
4. Huang D, Kraus WL. 2022 The expanding universe of PARP1-mediated molecular and therapeutic mechanisms. *Mol. Cell* **82**, 2315–2334. (doi:10.1016/j.molcel.2022.02.021)
5. Lüscher B, Bütepage M, Eckei L, Krieg S, Verheugd P, Shilton BH. 2018 ADP-ribosylation, a multifaceted posttranslational modification involved in the control of cell physiology in health and disease. *Chem. Rev.* **118**, 1092–1136. (doi:10.1021/acs.chemrev.7b00122)
6. Lüscher B *et al*. 2022 ADP-ribosyltransferases, an update on function and nomenclature. *Febs J.* **289**, 7399–7410. (doi:10.1111/febs.16142)
7. Palazzo L, Mikolčević P, Mikoč A, Ahel I. 2019 ADP-ribosylation signalling and human disease. *Open Biol.* **9**, 190041. (doi:10.1098/rsob.190041)
8. Catara G, Corteggio A, Valente C, Grimaldi G, Palazzo L. 2019 Targeting ADP-ribosylation as an antimicrobial strategy. *Biochem. Pharmacol.* **167**, 13–26. (doi:10.1016/j.bcp.2019.06.001)
9. Vyas S, Matic I, Uchima L, Rood J, Zaja R, Hay RT, Ahel I, Chang P. 2014 Family-wide analysis of poly(ADP-ribose) polymerase activity. *Nat. Commun.* **5**, 4426. (doi:10.1038/ncomms5426)
10. Groslambert J, Prokhorova E, Ahel I. 2021 ADP-ribosylation of DNA and RNA. *DNA Repair* **105**, 103144. (doi:10.1016/j.dnarep.2021.103144)
11. Rack JGM *et al*. 2024 Reversal of tyrosine-linked ADP-ribosylation by ARH3 and PARG. *J. Biol. Chem.* **300**, 107838. (doi:10.1016/j.jbc.2024.107838)
12. Schuller M *et al*. 2021 Molecular basis for DarT ADP-ribosylation of a DNA base. *Nature* **596**, 597–602. (doi:10.1038/s41586-021-03825-4)
13. Takamura-Enya T, Watanabe M, Totsuka Y, Kanazawa T, Matsushima-Hibiya Y, Koyama K, Sugimura T, Wakabayashi K. 2001 Mono(ADP-ribosyl)ation of 2′-deoxyguanosine residue in DNA by an apoptosis-inducing protein, pierisin-1, from cabbage butterfly. *Proc. Natl Acad. Sci. USA* **98**, 12414–12419. (doi:10.1073/pnas.221444598)

14. Leutert M *et al*. 2018 Proteomic characterization of the heart and skeletal muscle reveals widespread arginine ADP-ribosylation by the ARTC1 ectoenzyme. *Cell Rep.* **24**, 1916–1929. (doi:10.1016/j.celrep.2018.07.048)
15. Crawford K, Oliver PL, Agnew T, Hunn BHM, Ahel I. 2021 Behavioural characterisation of macrod1 and macrod2 knockout mice. *Cells* **10**, 368. (doi:10.3390/cells10020368)
16. Szántó M, Bai P. 2020 The role of ADP-ribose metabolism in metabolic regulation, adipose tissue differentiation, and metabolism. *Genes Dev.* **34**, 321–340. (doi:10.1101/gad.334284.119)
17. Rack JGM, Palazzo L, Ahel I. 2020 (ADP-ribosyl)hydrolases: structure, function, and biology. *Genes Dev.* **34**, 263–284. (doi:10.1101/gad.334631.119)
18. Schuller M *et al*. 2023 Molecular basis for the reversible ADP-ribosylation of guanosine bases. *Mol. Cell* **83**, 2303–2315. (doi:10.1016/j.molcel.2023.06.013)
19. Leidecker O *et al*. 2016 Serine is a new target residue for endogenous ADP-ribosylation on histones. *Nat. Chem. Biol.* **12**, 998–1000. (doi:10.1038/nchembio.2180)
20. Fontana P, Bonfiglio JJ, Palazzo L, Bartlett E, Matic I, Ahel I. 2017 Serine ADP-ribosylation reversal by the hydrolase ARH3. *eLife* **6**, 28533. (doi:10.7554/elife.28533)
21. Palazzo L, Leidecker O, Prokhorova E, Dauben H, Matic I, Ahel I. 2018 Serine is the major residue for ADP-ribosylation upon DNA damage. *eLife* **7**, 34334. (doi:10.7554/elife.34334)
22. Suskiewicz MJ *et al*. 2020 HPF1 completes the PARP active site for DNA damage-induced ADP-ribosylation. *Nature* **579**, 598–602. (doi:10.1038/s41586-020-2013-6)
23. Caggiano R *et al*. 2025 Suppression of ADP-ribosylation reversal triggers cell vulnerability to alkylating agents. *Neoplasia* **59**, 101092. (doi:10.1016/j.neo.2024.101092)
24. Slade D, Dunstan MS, Barkauskaite E, Weston R, Lafite P, Dixon N, Ahel M, Leys D, Ahel I. 2011 The structure and catalytic mechanism of a poly(ADP-ribose) glycohydrolase. *Nature* **477**, 616–620. (doi:10.1038/nature10404)
25. Sauve AA, Wolberger C, Schramm VL, Boeke JD. 2006 The biochemistry of sirtuins. *Annu. Rev. Biochem.* **75**, 435–465. (doi:10.1146/annurev.biochem.74.082803.133500)
26. Feldman JL, Baeza J, Denu JM. 2013 Activation of the protein deacetylase SIRT6 by long-chain fatty acids and widespread deacylation by mammalian sirtuins. *J. Biol. Chem.* **288**, 31350–31356. (doi:10.1074/jbc.C113.511261)
27. Jiang H *et al*. 2013 SIRT6 regulates TNF-α secretion through hydrolysis of long-chain fatty acyl lysine. *Nature* **496**, 110–113. (doi:10.1038/nature12038)
28. Bheda P, Jing H, Wolberger C, Lin H. 2016 The substrate specificity of sirtuins. *Annu. Rev. Biochem.* **85**, 405–429. (doi:10.1146/annurev-biochem-060815-014537)
29. Zhang X, Khan S, Jiang H, Antonyak MA, Chen X, Spiegelman NA, Shrimp JH, Cerione RA, Lin H. 2016 Identifying the functional contribution of the defatty-acylase activity of SIRT6. *Nat. Chem. Biol.* **12**, 614–620. (doi:10.1038/nchembio.2106)
30. Wang ZA *et al*. 2025 Structural and enzymatic plasticity of SIRT6 deacylase activity. *J. Biol. Chem.* **301**, 108446. (doi:10.1016/j.jbc.2025.108446)
31. Rossmann MG, Argos P. 1978 The taxonomy of binding sites in proteins. *Mol. Cell. Biochem.* **21**, 161–182. (doi:10.1007/BF00240135)
32. Avalos JL, Celic I, Muhammad S, Cosgrove MS, Boeke JD, Wolberger C. 2002 Structure of a Sir2 enzyme bound to an acetylated p53 peptide. *Mol. Cell* **10**, 523–535. (doi:10.1016/s1097-2765(02)00628-7)
33. Min J, Landry J, Sternglanz R, Xu RM. 2001 Crystal structure of a SIR2 homolog-NAD complex. *Cell* **105**, 269–279. (doi:10.1016/s0092-8674(01)00317-8)
34. Greiss S, Gartner A. 2009 Sirtuin/Sir2 phylogeny, evolutionary considerations and structural conservation. *Mol. Cells* **28**, 407–415. (doi:10.1007/s10059-009-0169-x)
35. Klein MA, Denu JM. 2020 Biological and catalytic functions of sirtuin 6 as targets for small-molecule modulators. *J. Biol. Chem.* **295**, 11021–11041. (doi:10.1074/jbc.REV120.011438)
36. Du J *et al*. 2011 Sirt5 is a NAD-dependent protein lysine demalonylase and desuccinylase. *Science* **334**, 806–809. (doi:10.1126/science.1207861)
37. Chen D *et al*. 2011 Identification of macrodomain proteins as novel O-acetyl-ADP-ribose deacetylases. *J. Biol. Chem.* **286**, 13261–13271. (doi:10.1074/jbc.M110.206771)
38. Zhu AY, Zhou Y, Khan S, Deitsch KW, Hao Q, Lin H. 2012 Plasmodium falciparum Sir2A preferentially hydrolyzes medium and long chain fatty acyl lysine. *ACS Chem. Biol.* **7**, 155–159. (doi:10.1021/cb200230x)
39. Rack JGM *et al*. 2015 Identification of a class of protein ADP-ribosylating sirtuins in microbial pathogens. *Mol. Cell* **59**, 309–320. (doi:10.1016/j.molcel.2015.06.013)
40. Ariza A, Liu Q, Cowieson NP, Ahel I, Filippov DV, Rack JGM. 2024 Evolutionary and molecular basis of ADP-ribosylation reversal by zinc-dependent macrodomains. *J. Biol. Chem.* **300**, 107770. (doi:10.1016/j.jbc.2024.107770)
41. García-Salcedo JA, Gijón P, Nolan DP, Tebabi P, Pays E. 2003 A chromosomal SIR2 homologue with both histone NAD-dependent ADP-ribosyltransferase and deacetylase activities is involved in DNA repair in *Trypanosoma brucei*. *EMBO J.* **22**, 5851–5862. (doi:10.1093/emboj/cdg553)
42. Kowieski TM, Lee S, Denu JM. 2008 Acetylation-dependent ADP-ribosylation by *Trypanosoma brucei* Sir2. *J. Biol. Chem.* **283**, 5317–5326. (doi:10.1074/jbc.M707613200)
43. Haigis MC *et al*. 2006 SIRT4 inhibits glutamate dehydrogenase and opposes the effects of calorie restriction in pancreatic beta cells. *Cell* **126**, 941–954. (doi:10.1016/j.cell.2006.06.057)
44. Mao Z, Hine C, Tian X, Van Meter M, Au M, Vaidya A, Seluanov A, Gorbunova V. 2011 SIRT6 promotes DNA repair under stress by activating PARP1. *Science* **332**, 1443–1446. (doi:10.1126/science.1202723)
45. Simonet NG *et al*. 2020 SirT7 auto-ADP-ribosylation regulates glucose starvation response through mH2A1. *Sci. Adv.* **6**, eaaz2590. (doi:10.1126/sciadv.aaz2590)
46. Mitra N, Dey S. 2020 Biochemical characterization of mono ADP ribosyl transferase activity of human sirtuin SIRT7 and its regulation. *Arch. Biochem. Biophys.* **680**, 108226. (doi:10.1016/j.abb.2019.108226)
47. Mostoslavsky R *et al*. 2006 Genomic instability and aging-like phenotype in the absence of mammalian SIRT6. *Cell* **124**, 315–329. (doi:10.1016/j.cell.2005.11.044)
48. Toiber D *et al*. 2013 SIRT6 recruits SNF2H to DNA break sites, preventing genomic instability through chromatin remodeling. *Mol. Cell* **51**, 454–468. (doi:10.1016/j.molcel.2013.06.018)
49. Van Meter M *et al*. 2016 JNK phosphorylates SIRT6 to stimulate DNA double-strand break repair in response to oxidative stress by recruiting PARP1 to DNA breaks. *Cell Rep.* **16**, 2641–2650. (doi:10.1016/j.celrep.2016.08.006)
50. Korotkov A, Seluanov A, Gorbunova V. 2021 Sirtuin 6: linking longevity with genome and epigenome stability. *Trends Cell Biol.* **31**, 994–1006. (doi:10.1016/j.tcb.2021.06.009)
51. Chio US, Rechiche O, Bryll AR, Zhu J, Leith EM, Feldman JL, Peterson CL, Tan S, Armache JP. 2023 Cryo-EM structure of the human Sirtuin 6-nucleosome complex. *Sci. Adv.* **9**, eadf7586. (doi:10.1126/sciadv.adf7586)
52. Rezazadeh S *et al*. 2020 SIRT6 mono-ADP ribosylates KDM2A to locally increase H3K36me2 at DNA damage sites to inhibit transcription and promote repair. *Aging* **12**, 11165–11184. (doi:10.18632/aging.103567)
53. Rezazadeh S, Yang D, Tombline G, Simon M, Regan SP, Seluanov A, Gorbunova V. 2019 SIRT6 promotes transcription of a subset of NRF2 targets by mono-ADP-ribosylating BAF170. *Nucleic Acids Res.* **47**, 7914–7928. (doi:10.1093/nar/gkz528)
54. Van Meter M, Kashyap M, Rezazadeh S, Geneva AJ, Morello TD, Seluanov A, Gorbunova V. 2014 SIRT6 represses LINE1 retrotransposons by ribosylating KAP1 but this repression fails with stress and age. *Nat. Commun.* **5**, 5011. (doi:10.1038/ncomms6011)
55. Simon M *et al*. 2022 A rare human centenarian variant of SIRT6 enhances genome stability and interaction with Lamin A. *EMBO J.* **41**, e110393. (doi:10.15252/embj.2021110393)
56. Zhang W *et al*. 2024 Sirt6 mono-ADP-ribosylates YY1 to promote dystrophin expression for neuromuscular transmission. *Adv. Sci.* **11**, 06390. (doi:10.1002/advs.202406390)

57. Crawford K, Bonfiglio JJ, Mikoč A, Matic I, Ahel I. 2018 Specificity of reversible ADP-ribosylation and regulation of cellular processes. *Crit. Rev. Biochem. Mol. Biol.* **53**, 64–82. (doi:10.1080/10409238.2017.1394265)
58. Cervantes-Laurean D, Minter DE, Jacobson EL, Jacobson MK. 1993 Protein glycation by ADP-ribose: studies of model conjugates. *Biochemistry* **32**, 1528–1534. (doi:10.1021/bi00057a017)
59. Daniels CM, Ong SE, Leung AKL. 2015 The promise of proteomics for the study of ADP-ribosylation. *Mol. Cell* **58**, 911–924. (doi:10.1016/j.molcel.2015.06.012)
60. Gibbs-Seymour I, Fontana P, Rack JGM, Ahel I. 2016 HPF1/C4orf27 is a PARP-1-interacting protein that regulates PARP-1 ADP-ribosylation activity. *Mol. Cell* **62**, 432–442. (doi:10.1016/j.molcel.2016.03.008)
61. Kar P *et al*. 2024 PARP14 and PARP9/DTX3L regulate interferon-induced ADP-ribosylation. *EMBO J.* **43**, 2929–2953. (doi:10.1038/s44318-024-00126-0)
62. Rack JGM, Zorzini V, Zhu Z, Schuller M, Ahel D, Ahel I. 2020 Viral macrodomains: a structural and evolutionary assessment of the pharmacological potential. *Open Biol.* **10**, 200237. (doi:10.1098/rsob.200237)
63. Liszt G, Ford E, Kurtev M, Guarente L. 2005 Mouse Sir2 homolog SIRT6 is a nuclear ADP-ribosyltransferase. *J. Biol. Chem.* **280**, 21313–21320. (doi:10.1074/jbc.M413296200)
64. Michishita E *et al*. 2008 SIRT6 is a histone H3 lysine 9 deacetylase that modulates telomeric chromatin. *Nature* **452**, 492–496. (doi:10.1038/nature06736)
65. Dominy JE Jr *et al*. 2012 The deacetylase Sirt6 activates the acetyltransferase GCN5 and suppresses hepatic gluconeogenesis. *Mol. Cell* **48**, 900–913. (doi:10.1016/j.molcel.2012.09.030)
66. Grimley R *et al*. 2012 Over expression of wild type or a catalytically dead mutant of Sirtuin 6 does not influence NFκB responses. *PLoS One* **7**, e39847. (doi:10.1371/journal.pone.0039847)
67. Larsen SC, Hendriks IA, Lyon D, Jensen LJ, Nielsen ML. 2018 Systems-wide analysis of serine ADP-ribosylation reveals widespread occurrence and site-specific overlap with phosphorylation. *Cell Rep.* **24**, 2493–2505. (doi:10.1016/j.celrep.2018.07.083)
68. Hendriks IA, Larsen SC, Nielsen ML. 2019 An advanced strategy for comprehensive profiling of ADP-ribosylation sites using mass spectrometry-based proteomics*. *Mol. Cell Proteomics* **18**, 1010–1026. (doi:10.1074/mcp.TIR119.001315)
69. Jankevicius G, Hassler M, Golia B, Rybin V, Zacharias M, Timinszky G, Ladurner AG. 2013 A family of macrodomain proteins reverses cellular mono-ADP-ribosylation. *Nat. Struct. Mol. Biol.* **20**, 508–514. (doi:10.1038/nsmb.2523)
70. Rosenthal F *et al*. 2013 Macrodomain-containing proteins are new mono-ADP-ribosylhydrolases. *Nat. Struct. Mol. Biol.* **20**, 502–507. (doi:10.1038/nsmb.2521)
71. Agnew T, Munnur D, Crawford K, Palazzo L, Mikoč A, Ahel I. 2018 MacroD1 is a promiscuous ADP-ribosyl hydrolase localized to mitochondria. *Front. Microbiol.* **9**, 20. (doi:10.3389/fmicb.2018.00020)
72. Sharifi R *et al*. 2013 Deficiency of terminal ADP-ribose protein glycohydrolase TARG1/C6orf130 in neurodegenerative disease. *EMBO J.* **32**, 1225–1237. (doi:10.1038/emboj.2013.51)
73. Đukić N *et al*. 2023 PARP14 is a PARP with both ADP-ribosyl transferase and hydrolase activities. *Sci. Adv.* **9**, eadi2687. (doi:10.1126/sciadv.adi2687)
74. Barkauskaite E *et al*. 2013 Visualization of poly(ADP-ribose) bound to PARG reveals inherent balance between exo- and endo-glycohydrolase activities. *Nat. Commun.* **4**, 2164. (doi:10.1038/ncomms3164)
75. Fontana P *et al*. 2023 Serine ADP-ribosylation in *Drosophila* provides insights into the evolution of reversible ADP-ribosylation signalling. *Nat. Commun.* **14**, 3200. (doi:10.1038/s41467-023-38793-y)
76. Palazzo L *et al*. 2015 Processing of protein ADP-ribosylation by Nudix hydrolases. *Biochem. J.* **468**, 293–301. (doi:10.1042/BJ20141554)
77. Minnee H, Chung H, Rack JGM, van der Marel GA, Overkleeft HS, Codée JDC, Ahel I, Filippov DV. 2023 Four of a kind: a complete collection of ADP-ribosylated histidine isosteres using Cu(I)- and Ru(II)-catalyzed click chemistry. *J. Org. Chem.* **88**, 10801–10809. (doi:10.1021/acs.joc.3c00827)
78. Minnee H, Rack JGM, van der Marel GA, Overkleeft HS, Codée JDC, Ahel I, Filippov DV. 2024 Solid-phase synthesis and biological evaluation of peptides ADP-ribosylated at histidine. *Angew. Chem. Weinheim Bergstr. Ger.* **136**, e202313317. (doi:10.1002/ange.202313317)
79. Bonfiglio JJ *et al*. 2017 Serine ADP-ribosylation depends on HPF1. *Mol. Cell* **65**, 932–940. (doi:10.1016/j.molcel.2017.01.003)
80. Prokhorova E *et al*. 2021 Unrestrained poly-ADP-ribosylation provides insights into chromatin regulation and human disease. *Mol. Cell* **81**, 2640–2655. (doi:10.1016/j.molcel.2021.04.028)
81. Hendriks IA *et al*. 2021 The regulatory landscape of the human HPF1- and ARH3-dependent ADP-ribosylome. *Nat. Commun.* **12**, 5893. (doi:10.1038/s41467-021-26172-4)
82. Pederson NJ, Diehl KL. 2025 DNA stimulates the deacetylase SIRT6 to mono-ADP-ribosylate proteins with histidine repeats. *J. Biol. Chem.* **301**, 108532. (doi:10.1016/j.jbc.2025.108532)
83. Zhong L *et al*. 2010 The histone deacetylase Sirt6 regulates glucose homeostasis via Hif1alpha. *Cell* **140**, 280–293. (doi:10.1016/j.cell.2009.12.041)
84. Sebastián C *et al*. 2012 The histone deacetylase SIRT6 is a tumor suppressor that controls cancer metabolism. *Cell* **151**, 1185–1199. (doi:10.1016/j.cell.2012.10.047)
85. Kanfi Y, Naiman S, Amir G, Peshti V, Zinman G, Nahum L, Bar-Joseph Z, Cohen HY. 2012 The sirtuin SIRT6 regulates lifespan in male mice. *Nature* **483**, 218–221. (doi:10.1038/nature10815)
86. Etchegaray JP *et al*. 2015 The histone deacetylase SIRT6 controls embryonic stem cell fate via TET-mediated production of 5-hydroxymethylcytosine. *Nat. Cell Biol.* **17**, 545–557. (doi:10.1038/ncb3147)
87. Kugel S *et al*. 2016 SIRT6 suppresses pancreatic cancer through control of Lin28b. *Cell* **165**, 1401–1415. (doi:10.1016/j.cell.2016.04.033)
88. Ferrer CM *et al*. 2018 An inactivating mutation in the histone deacetylase SIRT6 causes human perinatal lethality. *Genes Dev.* **32**, 373–388. (doi:10.1101/gad.307330.117)
89. Poltronieri P, Celetti A, Palazzo L. 2021 Mono(ADP-ribosyl)ation enzymes and NAD+ metabolism: a focus on diseases and therapeutic perspectives. *Cells* **10**, 128. (doi:10.3390/cells10010128)
90. Roichman A *et al*. 2021 Restoration of energy homeostasis by SIRT6 extends healthy lifespan. *Nat. Commun.* **12**, 3208. (doi:10.1038/s41467-021-23545-7)
91. Pan PW, Feldman JL, Devries MK, Dong A, Edwards AM, Denu JM. 2011 Structure and biochemical functions of SIRT6. *J. Biol. Chem.* **286**, 14575–14587. (doi:10.1074/jbc.M111.218990)
92. Bartlett E, Bonfiglio JJ, Prokhorova E, Colby T, Zobel F, Ahel I, Matic I. 2018 Interplay of histone marks with serine ADP-ribosylation. *Cell Rep.* **24**, 3488–3502. (doi:10.1016/j.celrep.2018.08.092)
93. Buch-Larsen SC, Hendriks IA, Lodge JM, Rykær M, Furtwängler B, Shishkova E, Westphall MS, Coon JJ, Nielsen ML. 2020 Mapping physiological ADP-ribosylation using activated ion electron transfer dissociation. *Cell Rep.* **32**, 108176. (doi:10.1016/j.celrep.2020.108176)
94. Leslie Pedrioli DM, Leutert M, Bilan V, Nowak K, Gunasekera K, Ferrari E, Imhof R, Malmström L, Hottiger MO. 2018 Comprehensive ADP-ribosylome analysis identifies tyrosine as an ADP-ribose acceptor site. *EMBO Rep.* **19**, e45310. (doi:10.15252/embr.201745310)
95. Palazzo L, Suskiewicz MJ, Ahel I. 2021 Serine ADP-ribosylation in DNA-damage response regulation. *Curr. Opin. Genet. Dev.* **71**, 106–113. (doi:10.1016/j.gde.2021.07.005)
96. Rack JGM *et al*. 2026 Supplementary material from: Histidine and Tyrosine Residues are Targets for SIRT6 ADP-ribosylation Activity. Figshare. (doi:10.6084/m9.figshare.c.8310073)